Title
FAST PROTONS FROM THE CAPTURE OF n-MESONS IN PHOTOGRAPHIC EMULSIONS

Author
Adelman, Frank L.

Publication Date
1950-11-15

UNCLASSIFIED

UCRL-2005

UNIVERSITY OF CALIFORNIA — BERKELEY

RADIATION LABORATORY

DISCLAIMER

UCRL-1005
Unclassified Distribution

UNIVERSITY OF CALIFORNIA

Radiation Laboratory

Contract No. W-7405-eng-48

Fast Protons from the Capture of π^--Mesons in Photographic Emulsions

Frank L. Adelman
(Ph.D. Thesis)
November 15, 1950

Berkeley, California

INSTALLATION	Number of Copies
Argonne National Laboratory	8
Armed Forces Special Weapons Project	1
Atomic Energy Commission - Washington	2
Battelle Memorial Institute	1
Brush Beryllium Company	1
Brookhaven National Laboratory	4
Bureau of Medicine and Surgery	1
Bureau of Ships	1
Carbide and Carbon Chemicals Division (K-25 Plant)	4
Carbide and Carbon Chemicals Division (Y-12 Plant)	4
Chicago Operations Office	1
Columbia University (J. R. Dunning)	1
Columbia University (G. Failla)	1
Dow Chemical Company	1
H. K. Ferguson Company	1
General Electric Company, Richland	3
Harshaw Chemical Corporation	1
Idaho Operations Office	1
Iowa State College	2
Kansas City Operations Branch	1
Kellex Corporation	2
Knolls Atomic Power Laboratory	4
Los Alamos Scientific Laboratory	3
Mallinckrodt Chemical Works	1
Massachusetts Institute of Technology (A. Gaudin)	1
Massachusetts Institute of Technology (A. R. Kaufmann)	1
Mound Laboratory	3
National Advisory Committee for Aeronautics	1
National Bureau of Standards	3
Naval Medical Research Institute	1
Naval Radiological Defense Laboratory	2
New Brunswick Laboratory	1
New York Operations Office	3
North American Aviation, Inc.	1
Oak Ridge National Laboratory	8
Patent Branch - Washington	1
Rand Corporation	1
Sandia Corporation	2
Santa Fe Operations Office	2
Sylvania Electric Products, Inc.	1
Technical Information Division (Oak Ridge)	15
Armament Division, Deputy for Research and Development (Capt. Glenn Davis)	1
Assistant for Atomic Energy, Deputy Chief of Staff (Col. Robert E. Greer)	1
Chief of Documents and Dissemination Branch (Col. J. E. Mallory)	1
USAF Assistant for Research Director of Research and Development, Deputy Chief of Staff (Col. B. G. Holzman)	1

INSTALLATION	Number of Copies
Electronic Systems Division (Mr. E. C. Trafton)	1
Chief of Scientific Advisors (Dr. Theodore von Karman)	1
USAF, Eglin Air Force Base (Major A. C. Field)	1
USAF, Kirtland Air Force Base (Col. Marcus F. Cooper)	1
USAF, Maxwell Air Force Base (Col. F. N. Moyers)	1
USAF, NEPA Office	2
USAF, Offutt Air Force Base (Col. H. R. Sullivan, Jr.)	1
USAF, Surgeon General, Medical Research Division (Col. A. P. Gagge)	1
USAF, Wright-Patterson Air Force Base (Rodney Nudenberg)	1
U. S. Army, Atomic Energy Branch (Lt. Col. A. W. Betts)	1
U. S. Army, Army Field Forces (Captain James Kerr)	1
U. S. Army, Commanding General, Chemical Corps Technical Command (Col. John A. MacLaughlin thru Mrs. Georgia S. Benjamin)	1
U. S. Army, Chief of Ordnance (Lt. Col. A. R. Del Campo)	1
U. S. Army, Commanding Officer, Watertown Arnsenal (Col. Carroll H. Deitrick)	1
U. S. Army, Director of Operations Research (Dr. Ellis Johnston)	1
U. S. Army, Office of Engineers (Allen O'Leary)	1
U. S. Army, Office of the Chief Signal Officer (Curtis T. Clayton thru Maj. George C. Hunt)	1
U. S. Army, Office of the Surgeon General (Col. W. S. Stone)	1
U. S. Geological Survey (T. B. Nolan)	2
U. S. Public Health Service	1
University of California at Los Angeles	1
University of California Radiation Laboratory	5
University of Rochester	2
University of Washington	1
Western Reserve University	2
Westinghouse Electric Company	4
R. F. Bacher (California Institute of Technology)	1
Cornell University	1
Total	140

Information Division
Radiation Laboratory
University of California
Berkeley, California

Fast Protons from the Capture of π^--Mesons in Photographic Emulsions

I.	Abstract	Page 3
II.	Introduction	4
III.	Theoretical	5
IV.	Experimental Arrangement	8
V.	Procedure	10
VI.	Errors	15
VII.	Results	16
VIII.	Discussion	21
IX.	Acknowledgements	28
X.	Mathematical Appendix	29
XI.	References	36

I. Abstract

The spectrum of fast protons from 1631 π^--meson absorptions in Ilford G-5 and C-2 emulsions has been studied. It has been found that (16.1 $\pm$ 1.8) percent of all π^--meson absorptions are accompanied by protons of energy greater than 20 Mev, and that (9.5 $\pm$ 1.3) percent of all absorptions are accompanied by protons of energy greater than 30 Mev. The proton energies were estimated by grain-counting in comparison with π^--mesons of known residual range. Allowance was made for the variation of grain density with position and depth in the emulsion. The energy spectrum is fairly flat from 30-70 Mev, but only three events were found above 70 Mev. Examination of stars from which the fast protons were emitted shows more prongs ejected opposite to the direction of the fast proton than are accounted for by evaporation from a recoiling nucleus. Comparison of the energy spectrum with the theoretical predictions permits the elimination of the various models in which the meson is captured by a proton of the nucleus and the recoil momentum is taken up by a single neighboring nucleon or by a triton. The spectrum favors the capture of the meson by a proton, with the recoil momentum taken by a small, variable number of nucleons. Furthermore, the evidence suggests that the low energy star prongs result from knock-on collisions of the primary nucleons with other nucleons inside the nucleus.

II. Introduction

There have been several attempts recently to discover the mechanism by which a π^--meson is captured by a complex nucleus. In the earliest models, the whole nucleus participated in the capture, and the entire rest mass of the π^--meson (about 140 Mev) was available for excitation of the nucleus. The evaporation models with an excitation energy of 140 Mev[1,2] fail to predict the observed energy spectrum[3,4] of the emitted charged particles. Furthermore, the observed average excitation energy of the meson stars was about 100 Mev,[3,4,5] considerably less than the total available energy. In 1949 Marshak[6] proposed a model in which the π^--meson interacts with a single proton of the nucleus, and the recoil momentum is taken up by a neighboring nucleon. The preliminary calculations indicated that more than 10 percent of the π^- absorptions should be accompanied by the emission of a proton of energy greater than 30 Mev. More detailed calculations by Fujimoto et al.[7] and by Tamor[8] supported this prediction. In order to check this prediction, the author,[9] Cheston and Goldfarb,[10] and Menon et al.[4] examined π^--meson endings in photographic emulsions capable of recording tracks of charged particles even at minimum ionization. They observed that fast protons* were indeed emitted from meson-induced stars, a result inconsistent with an evaporation process, but the data were too inconclusive to confirm or reject any of the specific hypotheses. The author's first study was essentially exploratory, with very

* In the rest of this paper, the term "fast proton" will refer to a proton of energy greater than 30 Mev.

few statistics and a crude method of energy estimation. Menon et al. and Cheston and Goldfarb had better statistics and more precise methods of energy determination. However, in each case the criterion of energy, the grain density, varied relatively slowly with proton energy in the neighborhood of 30 Mev. Furthermore, since the variation of observed grain density with position in the plate[11] and with depth in the emulsion was not taken into account, the number of protons of energy greater than 30 Mev could not be reliably determined.

It was felt, therefore, that a study of fast protons from π^--meson-induced disintegrations ought to be made, using large numbers of mesons and attempting to determine the energy spectrum more accurately.

III. Theory

The evaporation model for nuclear reactions is a statistical model, in which a compound nucleus is raised to a nuclear temperature by its energy of excitation and proceeds to "evaporate" particles, both charged and uncharged, until its temperature is reduced to a value too low to continue the emission process. In order to calculate the relation between temperature and excitation energy, a more specific nuclear model is required. The models which have been used most frequently are

(a) The Fermi gas model,[12,13] in which the interaction energy of the nucleons is small compared to their kinetic energy;

(b) The Fermi gas model with correlations[14] between the positions of the nucleons, as for electrons in metals;

(c) The liquid drop model,[15] in which the interaction energy of

the nucleons is large compared to their kinetic energy. Since this treatment is statistical, the conclusions are expected to be more valid for moderately heavy nuclei, such as Ag and Br, than for the lighter nuclei, such as C, N, and O. Therefore, some care must be used in applying these models to the stars found in photographic emulsions. However, as mentioned in Section II, it is difficult to reconcile these models with the observed mean excitation energy of π^--meson stars and with the observed energy spectrum of the star prongs.

The properties of Marshak's[6] model of π^--meson capture were first calculated in detail by Fujimoto et al.[7] The capture of the meson by a nuclear proton gives rise to a neutron of 70 Mev plus its Fermi energy, measured inside the nucleus, and a recoil proton or neutron of the same energy inside the nucleus. If either nucleon should collide with another nucleon before leaving the nucleus, its excess kinetic energy is considered to be given to the nucleus for the evaporation of particles. Therefore, the nucleus may have 0, 70, or 140 Mev excitation energy. This model predicts that a significant number of π^--meson absorptions should be accompanied by protons of 70 Mev;* in order to calculate the numerical percentage from the data given by the authors, assumptions must be made concerning the probability of charge exchange and the relative numbers of protons and neutrons available as the recoil particle. The results are given in Table I, where P(exch) is the probability that a neutron (proton) which escapes from the nucleus escapes as a proton (neutron) and n/p is the ratio of neutrons to

* If the collisions with smaller energy loss are taken into account, these protons should have a distribution of energies, almost all of them above 30 Mev.

protons available as the recoil particle.

Table I

Percentage of π^--Meson Absorptions Accompanied by a Fast Proton		
P(exch)	n/p = 1	n/p = 2
0	17.4	11.6
1/4	24.7	22.1
1/3	27.1	25.4
1/2	32.0	32.0
1	46.5	50.5

Meanwhile, Tamor[8] made similar calculations using two different models. I. The recoil momentum is taken up by a single nucleon, as above, which has twice the probability of being a neutron as a proton, on the basis of the α-particle model of nuclei. II. The recoil momentum is taken up by the residual triton which remains after a proton of an α-particle captures the meson. This gives a 31 Mev triton, whose energy goes into nuclear excitation energy, and one 95 Mev neutron, if the π^--meson has a mass of 286 times the electron mass. The calculations were made for nitrogen and silver nuclei under the following assumptions:

(1) All nucleons in the nucleus are initially at rest;

(2) They collide inside the nucleus as free nucleons;

(3) In each collision 25 Mev is given to the nucleus for excitation, but the nucleon is undeviated;

(4) A nucleon of energy less than 30 Mev is indistinguishable from an evaporated nucleon;

(5) In each neutron-proton collision the probability of exchange is 1/2.

The number of fast protons predicted by these models is given in Table II.

Table II

Percentage of π^--Meson Absorptions Accompanied by a Fast Proton		
Model	Ag	N
I	24	48
II	13	12

Model II also predicts that 52 percent* of the π^- absorptions should show no charged particles except possibly recoil nuclei, while Model I predicts 38 percent, more nearly in agreement with the work of Adelman and Jones[16] and of Menon et al.[4]

More recently Fujimoto, Takayanagi, and Yamaguchi[17] proposed to account for the fast protons without the assumption of a recoil triton. By allowing for the momentum distribution of the nucleons inside the nucleus in the calculations of Fujimoto et al.,[7] they concluded that about 19 percent of the π^--meson absorptions in heavy nuclei should be accompanied by fast protons up to 136 Mev, with a peak around 65 Mev.

IV. Experimental Arrangement

The photographic plates were exposed in the 184-inch Berkeley cyclotron as shown in Figure 1. They were put a relatively large distance from the target in order to reduce the background due to

* On the basis that 54 percent of the π^--mesons are captured in heavy elements of the emulsion, as shown in Menon et al.[4]

neutral particles from the target. At this distance most of the mesons which could reach the plates had enough energy (~ 30 Mev or more) to pass completely through the pack of plates. Therefore a 3/8-inch aluminum absorber was placed in front of the plates to slow down the mesons. With this arrangement, about 2500 mesons were found to end in a 1-inch x 3-inch x 200μ emulsion with an exposure of 10 seconds to a 345 Mev proton beam current of about $1/2 \times 10^{-6}$ ampere. The 200μ thickness was chosen in order to record a sufficiently long segment of a fast proton and still to retain ease of scanning and development.

Ilford G-5 emulsions were chosen for this experiment so that the most energetic protons might be observed. Since these plates had acquired a heavy background of low energy electrons by the time they had reached Berkeley, it was desirable to eradicate the latent images by accelerated fading.[18] By storing the plates in an oven at about 33°C over a pan of water for about 50 hours and then drying, it has been found possible to eliminate 90 percent of the latent image electrons without any noticeable loss of sensitivity. The plates were exposed and developed as soon as possible after the background eradication.

Shortly after work was begun on this project, however, it was found from the variation of the grain density with meson residual range that the grain density in G-5 emulsions was a slowly varying function of proton energy below 40 Mev. Therefore, the proton spectrum below 60 Mev was examined in the less sensitive Ilford G-2 emulsions, which, incidentally, require no eradication.

V. Procedure

The plates were scanned with an 8-mm apochromatic objective and 5x compensated eyepieces, giving a total magnification of 100x. Afterwards each meson ending was examined with a 1.8-mm apochromatic oil immersion objective and the same eyepieces, a magnification of 475x. The number of prongs of each star was ascertained, and the presence of lightly ionizing tracks emanating from the meson terminus was noted. Each of the lightly ionizing heavy particle tracks was grain-counted with the oil immersion objective and 25x compensated eyepieces. In order to get maximum resolution, oil was used between the condenser lens and the photographic plates.

Grain counts were made over 43μ segments. To establish the variation of grain density with energy, mesons were grain-counted in the following manner. Using the range-energy relation for protons in Ilford emulsion[19] and the ratio of masses of π^--meson and proton,[20] a table was made of meson residual range and the energy of a proton of the same velocity. Since a meson of 3.7 mm residual range has the same velocity as a 90 Mev proton, mesons which remained in the emulsion for 4 mm from their termini were quite satisfactory.

Six favorable star-forming mesons in G-5 plate No. 22212 were chosen, and grain counts were taken at meson velocities corresponding to proton energies from 45 Mev to 90 Mev at approximately 5 Mev intervals. For each velocity, three consecutive 43μ segments of each meson were counted. The depth in the emulsion of the center of the middle segment of each group of three segments was taken as the mean depth of each group. This procedure does not introduce appreciable error, as

the mesons chosen were almost parallel to the emulsion surface. Since each segment corresponded to a different proton energy, the residual ranges of the mesons were used to find the energy corresponding to each segment.

The data were divided into six groups (A, B,..,F) according to depth in the emulsion. At each 5 Mev point the average differential grain count for each group was plotted against $\frac{1}{\sqrt{E_p}}$, where E_p is the energy of a proton of the same velocity as the meson at the central point of the three corresponding segments. The plot is shown in Figure 2. Since it is reasonable to consider the six sets of points as straight lines with roughly the same slope, it follows that, to a good approximation, the differential grain count may be treated as the product of 2 factors, one depending only upon energy and the other, only upon depth.

Therefore the grain density for group C (20-42μ in depth), the most numerous group, was plotted against $\frac{1}{\sqrt{E_p}}$, using the proper energy for each segment; the best straight line, in the sense of least squares, was determined assuming that the error in $\frac{1}{\sqrt{E_p}}$ is small compared to that in the differential grain count. This plot, shown in Figure 3, determined the grain density as a function of energy. The scatter of the points in this figure is not a valid measure of the error in the straight line, as each point corresponds to a single 43μ segment, while there were two to four segments counted at each energy used for constructing the line. In order to find the dependence upon depth, the grain density for all the other segments was divided by the corresponding grain density as read from the line, and the arithmetic mean of the ratios was plotted for each group against the central depth of that

group (Figure 4). A straight line fit for the four intermediate points was assumed for simplicity; the two extreme points were considered unreliable, due to insufficient data and large fluctuations in the ratios in these two groups. All segments within 10μ after development of either emulsion surface were discarded.

A similar procedure was used for C-2 plate No. 22886. However, the meson velocities used corresponded to proton energies from 20 Mev up. The least squares straight line for these grain counts is shown in Figure 5, and the variation with depth is given in Figure 6. It should be noticed that the depth variation is considerably smaller for the C-2 plate than for the G-5 and is in the opposite direction. This is due to the use of a temperature development technique* similar to one suggested by Winand.[21] The warm stage of the development took place in water, and diffusion of developer outward probably accounts for the observed variation. It should also be mentioned that the data and observed fluctuations of meson grain counts in the C-2 plates justified retaining particles within 10μ (developed) of the glass, but not of particles near the emulsion-air surface.

In the two G-5 plates used the variation of grain density with depth in the emulsion was assumed to be the same, since they were developed simultaneously. However, in order to allow for variation of sensitivity between the two plates, one meson on plate No. 22009 was counted as above, and found to have an average grain density, after

* One hour soak in H_2O at 5°C; two hour immersion at 5°C in one part of D-19 diluted by six parts of H_2O; immersion in H_2O at 5°C, raising temperature to 20°C in twenty minutes; fixing.

correction for depth in the emulsion, of about one grain less per 43μ than the average for the other G-5 plate. Since this is considerably less than the standard deviation of the grain counts, it was felt that further grain counting on mesons in this plate was not worth while. Instead, a correction of + 1 grain per 43μ was applied to the grain counts of the protons in that plate.

Another factor which affects the apparent grain count is the angle between the track and its projection upon the plane of the emulsion. Obviously, a steep track will have more grains per unit projected length than a gently sloping track of the same velocity. In order to correct for this, the ratio of the undeveloped to the developed thickness of the plates must be estimated. This ratio, which is called the shrinkage factor, is a function of the emulsion type, the processing, and the relative humidities at the time of exposure and after development. Therefore the ratio should be determined at each laboratory, rather than by taking a figure from the literature. The relative humidity at the time of observation is unimportant, as the plates are protected by a mixture of Duco cement and lacquer thinner* in order to keep the emulsion from peeling. With this coating the developed thickness was observed to vary by only ± 1-1/2 percent over a period of several months. The shrinkage factor for this experiment has been taken as 2.4 ± 0.1.[22] The undeveloped emulsion thickness has been found to vary as much as ± 20 percent from that given by the manufacturer, and therefore cannot be used to compute this ratio. Using this factor, the

* Developed by D. J. O'Connell.

grain counts must be multiplied by the cosine of the angle between the original direction of the track and its projection. This angle is measured under the assumption that the track does not scatter appreciably before leaving the emulsion, an assumption which is most valid for the shorter and, therefore, steeper tracks.

At large angles, the apparent overlapping of the grains of the track, the short track length available for counting, and the large uncertainty in the cosine of the angle all combine to increase the uncertainty in the grain count. Therefore a minimum projected track length of 86μ (= 2 reticule lengths) was arbitrarily chosen as the shortest track which was to be counted. Furthermore, only tracks which traveled at angles less than 45° from the plane of the emulsion were used. Naturally, corrections must be made for these omissions. These corrections, which are calculated in Section X, are of the order of 40 percent.

Other data were excluded also. Those meson stars which lay within 5μ after development (= 12μ before development) of either emulsion surface were discarded, since otherwise one or more prongs of a star might be missed. In addition, all stars within 3 mm of an edge of the plate were discarded, as the grain density in this region is higher than normal and varies rapidly with position.[11] Furthermore, since grain counts within 10μ after development of either emulsion surface in G-5 plates (or within 10μ of the emulsion-air surface in the C-2 plate) were not felt to be reliable, as mentioned above, all segments of track which lay closer than this distance were not included. A correction factor of the order of 1-1/2 percent is calculated in

Section X in order to account for those protons which lie completely within 10μ of an emulsion surface and are not otherwise excluded.

No correction was made, however, for random grain background in the plates. Such a correction is unnecessary, as particles of the same velocity are being compared in the same plates with the same background. On the other hand, at low grain densities, statistical fluctuations in the number of background grains that are confusable with grains of a track become important; furthermore, the number of confusable grains increases as the distance between the grains increases. Therefore, in the C-2 plates observations were restricted to protons of grain density higher than 24.6 grains per 43μ (equivalent to protons of energy less than 60 Mev).

VI. Errors

The errors in the determination of the energy of the protons are statistical in nature. The standard deviation of the grain count of a single 43μ segment of meson or proton track was taken as[23]

$$\sigma = \sqrt{N\left(1 - \frac{N}{129}\right)}$$

as shown in Section X, where N is the number of grains in the segment. Since $36 \leq N \leq 78$ in the G-5 plates, $5.1 \leq \sigma \leq 5.7$, while the root mean square deviation of the points in Figure 3 from the least squares line is about 5. Similarly, in the C-2 plate, $15 \leq N \leq 54$, and $3.8 \leq \sigma \leq 5.6$, while the r.m.s. deviation in Figure 5 is about 4. These figures imply that variations in sensitivity over the plates have a negligible effect upon the grain counts, and that the errors in the grain counts are

essentially random.

The standard deviation, σ_1, due to uncertainty in the least squares fit is of the order of 1/2 grain to 1 grain per 43μ (see Figures 7 and 8). In the computation of the standard deviation of the grain counts, σ_1 was taken as ± 1 grain per 43μ. The calculations which led to these figures are given in Section X.

The largest error in the energy estimation is the standard deviation of the proton grain counts. This is given by (see Section X):

$$\sigma_2 = \sqrt{\frac{\bar{N}}{n}\left(1 - \frac{\bar{N}}{129}\right)} \cos \phi,$$

where n is the number of 43μ segments counted, $\bar{N}$ is the mean number of grains per segment, and ϕ is the angle between the track and its projection upon the plane of the emulsion. In general, σ_2 is of the order of ± 2 grains per 43μ.

Other errors, both of the order of ± 1 grain per 43μ, are due to the uncertainty of the variation of grain density with depth in the emulsion (σ_3), and, for protons in plate No. 22009, to the uncertainty in the relative sensitivities of plates No. 22009 and No. 22212 (σ_4).

Since all these errors are independent, the standard deviation at 30 Mev is of the order of ± 2-1/2 grains per 43μ or ± 4 Mev. At higher energies, the error is somewhat higher. Therefore, the precision in the number of fast protons above 30 Mev is relatively high and is limited mainly by the small number of events.

VII. Results

A total of 1631 meson absorptions were examined, 992 in G-5 emul-

sion and 639 in C-2 emulsion. The observed protons* of energy greater than 20 Mev are listed in Table III. Typical examples and grain densities are given in Figures 9 and 10. The energy spectrum of these protons, before and after the application of the geometrical corrections, is shown in Figure 11; the number of prongs per star is given in Figure 12 (no geometrical correction has been applied to these data). After the corrections are applied, (16.1 ± 1.8) percent of all meson absorptions are accompanied by protons of energy greater than 20 Mev, and (9.5 ± 1.3) percent of all absorptions are accompanied by protons of energy greater than 30 Mev. In terms of ejected particles, (10.3 ± 1.2) percent of all star prongs are protons of energy greater than 20 Mev, and (6.0 ± 0.8) percent are protons of energy greater than 30 Mev. These numbers are in agreement with those of other workers.[4,10]

A precise prong spectrum** for meson induced stars may also be given by use of the data of this study. Since Adelman and Jones[16] and Menon et al.[4] used the same conventions*** for star prongs as the author, their data may be combined with that found here to give the prong spectrum of Table IV, based upon 3366 meson stars.

---

* The grain density of a 20 Mev proton is equal to that of a 40 Mev deuteron or of a 60 Mev triton. Therefore the term "proton" includes deuterons of twice the energy and tritons of three times the energy in question. The few cases where positive identification can be made from the range of the particles are mentioned in Table III.

** i.e., the frequency distribution of stars of a given number of prongs.

*** Any group of grains (except an electron track) leaving the terminus of a meson with a well-defined direction is a star prong.

Table III

Event	Grain Count to Nearest 1/2 Grain per 43μ	Proton Energy (Mev)	Total Number of Prongs of Associated Star	Remarks
1	42 ± 5	85^{+18}_{-11}	2	
2	46 ± 2-1/2	$76.1^{+6.1}_{-5.5}$	2	
3	46 ± 3-1/2	$76.1^{+8.0}_{-7.5}$	3	
4	49 ± 2	$69.6^{+4.3}_{-3.8}$	1	
5	49 ± 3	$69.6^{+6.5}_{-5.8}$	2	
6	50-1/2 ± 4	$66.8^{+8.2}_{-7.6}$	1	
7	51 ± 3	$65.8^{+5.9}_{-5.6}$	2	
8	52 ± 4-1/2	$63.8^{+9.0}_{-7.5}$	3	
9	53 ± 3	$61.9^{+5.8}_{-4.7}$	2	
10	53 ± 3	$61.9^{+5.8}_{-4.7}$	1	
11	53-1/2 ± 3	$61.1^{+5.7}_{-4.8}$	1	
12	55 ± 3	$58.7^{+5.1}_{-4.4}$	2	
13	25 ± 2	$58.5^{+8.9}_{-7.3}$	3	
14	25 ± 2	$58.5^{+8.9}_{-7.3}$	2	
15	55-1/2 ± 3	$58.0^{+4.8}_{-4.2}$	4	
16	55-1/2 ± 3	$58.0^{+4.8}_{-4.2}$	3	
17	25-1/2 ± 2	$56.5^{+8.5}_{-6.9}$	3	
18	25-1/2 ± 2-1/2	$56.5^{+10.9}_{-8.4}$	1	
19	56-1/2 ± 3	$56.3^{+4.8}_{-4.1}$	4	
20	57-1/2 ± 3	$55.0^{+4.4}_{-4.1}$	1	
21	58 ± 3	$54.3^{+4.4}_{-4.1}$	4	
22	58 ± 4	$54.3^{+5.9}_{-5.2}$	2	

Event	Grain Count to Nearest 1/2 Grain per 43μ	Proton Energy (Mev)	Total Number of Prongs of Associated Stars	Remarks
23	58-1/2 ± 5-1/2	$53.8 \pm \frac{8.1}{7.2}$	1	
24	26-1/2 ± 2-1/2	$52.9 \pm \frac{9.7}{7.5}$	2	
25	60 ± 2-1/2	$51.5 \pm \frac{3.5}{3.0}$	2	
26	60 ± 3	$51.5 \pm \frac{4.0}{3.7}$	1	
27	60 ± 4-1/2	$51.5 \pm \frac{6.5}{5.4}$	2	
28	27 ± 2-1/2	$51.2 \pm \frac{9.3}{7.2}$	2	
29	27 ± 2-1/2	$51.2 \pm \frac{9.3}{7.2}$	3	
30	28 ± 2	$48.1 \pm \frac{6.5}{5.5}$	1	
31	28 ± 2-1/2	$48.1 \pm \frac{8.4}{6.6}$	1	
32	28 ± 2-1/2	$48.1 \pm \frac{8.4}{6.6}$	3	
33	28-1/2 ± 2-1/2	$46.6 \pm \frac{8.0}{6.3}$	1	
34	28-1/2 ± 2-1/2	$46.6 \pm \frac{8.0}{6.3}$	3	
35	29 ± 2-1/2	$45.4 \pm \frac{7.5}{6.2}$	2	
36	30 ± 2-1/2	$42.6 \pm \frac{7.0}{5.5}$	2	
37	30 ± 2-1/2	$42.6 \pm \frac{7.0}{5.5}$	1	
38	30-1/2 ± 2-1/2	$41.5 \pm \frac{6.6}{5.5}$	3	
39	31 ± 2-1/2	$40.3 \pm \frac{6.3}{5.2}$	2	
40	31-1/2 ± 2-1/2	$39.2 \pm \frac{6.2}{5.0}$	2	
41	32 ± 2-1/2	$38.1 \pm \frac{5.9}{4.8}$	2	
42	32 ± 2-1/2	$38.1 \pm \frac{5.9}{4.8}$	2	
43	32 ± 3	$38.1 \pm \frac{7.3}{5.6}$	3	
44	32-1/2 ± 2-1/2	$37.1 \pm \frac{5.5}{4.6}$	1	
45	33 ± 2	$36.0 \pm \frac{4.3}{3.5}$	2	

Event	Grain Count to Nearest 1/2 Grain per 43μ	Proton Energy	Total Number of Prongs of Associated Star	Remarks
46	33-1/2 ± 2-1/2	$35.1 \pm \frac{5.2}{4.2}$	5	
47	34 ± 2-1/2	$34.2 \pm \frac{5.0}{4.1}$	3	
48	34 ± 2-1/2	$34.2 \pm \frac{5.0}{4.1}$	3	
39	34 ± 3-1/2	$34.2 \pm \frac{7.3}{5.5}$	1	
50	35-1/2 ± 2-1/2	$31.7 \pm \frac{4.3}{3.7}$	4	
51	35-1/2 ± 3	$31.7 \pm \frac{5.4}{4.3}$	2	
52	36-1/2 ± 5	$30.1 \pm \frac{9.1}{6.2}$	2	
53	37 ± 2	$29.4 \pm \frac{3.1}{2.6}$	4	
54	37-1/2 ± 2-1/2	$28.7 \pm \frac{3.8}{3.1}$	3	From same star as No. 64
55	37-1/2 ± 3-1/2	$28.7 \pm \frac{5.5}{4.3}$	1	
56	38 ± 2-1/2	$28.0 \pm \frac{3.7}{3.0}$	3	
57	38 ± 2-1/2	$28.0 \pm \frac{3.7}{3.0}$	2	
58	38 ± 2-1/2	$28.0 \pm \frac{3.7}{3.0}$	1	
59	38 ± 2-1/2	$28.0 \pm \frac{3.7}{3.0}$	2	
60	38 ± 2-1/2	$28.0 \pm \frac{3.7}{3.0}$	2	~54 Mev deuteron by range
61	39 ± 2-1/2	$26.8 \pm \frac{3.3}{2.9}$	2	
62	39 ± 2-1/2	$26.8 \pm \frac{3.3}{2.9}$	5	
63	39-1/2 ± 2	$26.2 \pm \frac{2.5}{2.3}$	3	
64	39-1/2 ± 2-1/2	$26.2 \pm \frac{3.2}{2.8}$	3	~26 Mev proton by range From same star as No. 54
65	41 ± 2-1/2	$24.4 \pm \frac{3.0}{2.5}$	2	
66	41 ± 2-1/2	$24.4 \pm \frac{3.0}{2.5}$	1	

Event	Grain Count to Nearest 1/2 Grain per 43μ	Proton Energy	Total Number of Prongs of Associated Star	Remarks
67	41 ± 2-1/2	$24.4 \pm^{3.0}_{2.5}$	3	~23 Mev proton by range
68	41-1/2 ± 2	$23.9 \pm^{2.3}_{2.0}$	2	
69	41-1/2 ± 3-1/2	$23.9 \pm^{4.1}_{2.5}$	3	
70	42 ± 2-1/2	$23.4 \pm^{2.8}_{2.3}$	2	
71	42 ± 3-1/2	$23.4 \pm^{4.0}_{3.2}$	3	
72	42 ± 3-1/2	$23.4 \pm^{4.0}_{3.2}$	1	
73	43 ± 2-1/2	$22.4 \pm^{2.6}_{2.2}$	4	
74	44 ± 2	$21.5 \pm^{1.9}_{1.7}$	4	
75	44 ± 2-1/2	$21.5 \pm^{2.4}_{2.1}$	3	
76	44 ± 2-1/2	$21.5 \pm^{2.4}_{2.1}$	3	
77	44 ± 3	$21.5 \pm^{2.9}_{2.5}$	1	
78	44 ± 3	$21.5 \pm^{2.9}_{2.5}$	2	
79	45 ± 2-1/2	$20.6 \pm^{2.3}_{1.9}$	2	

Table IV

Number of prongs	1	2	3	4	5	6
Percent of stars	32.4±1.0	32.7±1.0	22.3±0.8	10.5±0.6	2.0±0.2	0.1±0.1

VIII. Discussion

An analysis of the results and figures of Section VII will be made in this section in order to show that the evaporation model fails to explain the results of the secondary process in meson absorption. An

alternative model will be proposed at the end of this section.

First, however, the models of the primary interaction will be eliminated as far as possible on the basis of the data of this study. The two-nucleon model of π^--meson capture calculated by Fujimoto et al.[7] predicts at least twice as many fast protons as are observed (cf. Table I), unless it is assumed that the probability of charge exchange is less than 1/4 and that the neutron-proton ratio for the recoil particle is at least 2. Even then, the predicted number is higher than that observed. The next calculations of Fujimoto and his co-workers,[17] in which the momentum distribution of the nucleons is taken into account, predict entirely too many fast protons (19 percent), a peak in the energy spectrum at 65 Mev (which is not observed), and a spectrum extending up to 136 Mev. Since the two calculations were made only for heavy nuclei, the conclusions as to the validity of the proposed models must be somewhat conservative. Still, the predictions of the latter calculations are in definite contradiction with the observed energy spectrum, and the former model of Fujimoto et al.[7] stands on a rather tenuous basis.

Tamor's[8] model I predicts many too many fast protons, as pointed out by Menon et al.[4] and by Cheston and Goldfarb,[10] and his α-particle model (II) is also generous in its predicted number of fast protons (see Table II). Furthermore, model II predicts too low an excitation energy (55-70 Mev) and too many starless meson absorptions. However, this calculation assumed that the scattering cross sections for like particles were 1/4 those for unlike particles. The calculation for equal cross sections, which is more nearly in accord with the high

energy p-p and n-p scattering data,[24] leads to results which are more nearly in agreement with experimental data, as mentioned in a footnote in reference 8. But this model assumes that there is a 95 Mev neutron traveling inside the nucleus and escaping as a proton about 12 percent of the time. In this case, one expects a larger number of protons between 70 and 95 Mev than is actually observed. Thus Tamor's two-nucleon model may be eliminated, and his α-particle model may probably be rejected. Incidentally, the ratio of fast protons from heavy elements to those from light elements as observed in the paper of Menon et al.[4] is not a completely valid objection to the α-particle model of Tamor. Their results using the potential barrier method to separate the stars are not consistent with their observations with sandwich plates (cf. Menon's Table IV with his discussion on page 591 and with his Table V). Since the stars with energetic protons may have different prong characteristics than the other stars, the method is felt to be unreliable. Therefore, no attempt was made to distinguish the absorptions in heavy elements from those in light elements.

Another proposal was made by Menon et al.[4] They assumed that the primary interaction takes place among 3 or 4 nucleons, and that the energy of those nucleons which do not escape is used in heating the nucleus. For their preliminary calculations, they assumed an α-particle model, for which calculations had been made by Ruddlesden and Clark.[25] The predictions of this preliminary computation are an excitation energy of 120 Mev, which is somewhat high, and a peak in the number of protons between 30 and 40 Mev, for which there is no evidence in Figure 11. However, when the interactions of the smaller numbers of nucleons

are taken into account, the mean excitation energy should decrease and the peak should be smoothed out. Thus their proposed model is not inconsistent with the spectrum of Figure 11.

Proceeding now to the discussion of the general features of the data of this study, we shall look more closely at Figure 11. As may be seen from this figure, the number of protons in the range 20-30 Mev is twice the number in the range 30-40 Mev. Since a 20 Mev proton could reasonably have come from a nuclear evaporation with excitation energy of 100 Mev, while a proton of 30 Mev is much less likely to have come from such a process, the energy spectra of the protons from the primary and secondary processes overlap considerably. This implies either that relatively low energy primary nucleons occur often or that some of the lower energy protons are knock-on particles from collisions with high energy primary nucleons.

Another characteristic of the energy spectrum is that the number of protons decreases slowly with energy in the range 30-70 Mev, and drops off above 70 Mev; there are fewer protons of energy greater than 70 Mev than there are in any 5 Mev interval below 70 Mev. Thus relatively few of the π^- absorptions take place with the creation of a primary nucleon of energy greater than 70 Mev, while nucleons occur often with energies lower than this figure. Therefore the primary act must take place often among two or more nucleons, with a deuteron or triton seldom acting alone as the recoil particle. On the other hand, three of the events listed in Table III ended in the emulsion. Two of these were actually protons by range and grain density, and the third was a 54 Mev deuteron. In addition, one particle was found which was

probably a triton of 30 Mev, and another was either a 23 Mev proton with abnormally high grain density or a 31 Mev deuteron with abnormally low grain density. Neither of these particles is included in Table III. Thus it appears that deuterons and tritons actually take part in the primary process; if they were knock-on particles, the energetic primaries required would lead to a larger number of protons of energy greater than 50 Mev than in the range 30-50 Mev,[26] in contradiction to Figure 11. This conclusion does not contradict the earlier conclusion of this paragraph, since there is not enough data to observe the relative numbers of protons, deuterons, and tritons.

From Figure 12, it may be seen that the prong spectrum of the stars in Figure 12 (after applying geometrical corrections) is consistent with that of the whole group of stars examined and with Table IV. This implies that most of the π^- absorptions which are not accompanied by protons of energy greater than 20 Mev are accompanied by neutrons of similar energies. This would seem to indicate that the number of neutrons available as the recoil particle is twice the number of available protons (since one neutron is always involved), as in the α-particle model of nuclei. There are, however, a number of considerations which weaken this conclusion:

(a) The statistics for the comparison of prong spectra are poor;

(b) The prong distribution for stars with energetic protons cannot strictly be compared with that for other stars, for the former stars include an extra prong per star (the energetic proton). On the other hand, the residual nucleus for the latter stars has an extra proton and one neutron too few,

favoring the emission of a proton over the emission of a neutron. These two effects tend to cancel;

(c) Charge exchange tends to equalize the numbers of energetic protons and neutrons emitted. Thus more protons are observed than are involved in the primary interaction. However, this effect should be partly or wholly compensated for by

(d) The potential barrier, which has an appreciable effect upon the emission from heavy nuclei of 20 Mev protons relative to neutrons involved in the primary process.

It still appears reasonable, however, to state that the evidence favors the ratio of 2:1 for neutrons to protons available as the recoil particle.

The most interesting feature of the data appeared upon an examination of the stars associated with the energetic protons. A very pronounced asymmetry was observed in the angular distribution of the star prongs emitted in addition to a proton of energy greater than 20 Mev. As may be seen from Table V below, the observed asymmetry between the backward and forward hemispheres (with respect to the energetic proton) is significantly higher than that calculated with very generous assumptions, ascribing the asymmetry to the motion of the recoiling nucleus. The asymmetry is calculated assuming that the residual nucleus has a mass twelve times that of a proton, and the outgoing particles are assumed to have the lowest velocity which is used in measuring the asymmetry. All particles are assumed to be either protons or α-particles. In Table V, the following symbols are used:

E_p: The energy of the slowest secondary proton considered in measuring the asymmetry.

$c\beta(E_p)$: The velocity of a proton of energy E_p or of an α-particle of the same range (i.e., of energy $4E_p$).

$\bar{E}$: The mean energy of the observed protons whose associated star prongs are used in measuring the asymmetry.

$c\beta(\frac{\bar{E}}{144})$: The velocity of the nucleus mentioned above recoiling from the emission of a proton of energy $\bar{E}$.

R_{calc}: The ratio of the number of secondary star prongs expected with a component of velocity in the direction opposite to that of the energetic proton to the number expected with a component in the direction of the proton.

R_{obs}: The observed ratio.

The derivation of R_{calc} is given in Section X.

Table V

E_p(Mev)	$\beta(E_p)$	$\bar{E}$(Mev)	$\beta(\frac{\bar{E}}{144})$	R_{calc}	R_{obs}
4	0.0924	56.8	0.0290	1.92:1	6:0
		43.8	0.0253	1.75:1	9:2
		23.2	0.0185	1.50:1	5:1
2	0.0654	56.3	0.0288	2.58:1	8:0
		41.6	0.0248	2.22:1	12:5
		24.1	0.0187	1.81:1	10:2
1	0.0462	56.3	0.0288	4.57:1	9:0
		42.6	0.0251	3.38:1	14:5
		24.5	0.0188	2.37:1	16:3

The disagreement between R_{obs} and R_{calc} is striking, and leads immediately to an alternative model: The secondary star prongs are assumed to be due mainly to impacts with primary nucleons traveling through the nucleus. Seldom would a particle be expected to be emitted

in the direction of an emitted fast proton. However, one can no longer assume that there are two 70 Mev nucleons traveling in opposite directions, for then the observed energy spectrum would have more high energy protons.[26]

Therefore it is proposed that the primary interaction take place among a small, but variable, number of nucleons (most often 2, 3, or 4), as in Menon et al.[4] This permits the emission of protons up to 70 Mev with reasonable probability, and protons up to 95 Mev occasionally. These nucleons have a spread of energies which favors the emission of low energy knock-on particles. Since the mean free path of such a nucleon is of the order of the nuclear radius for an element like Ag,[26] each nucleon will collide, on the average, one time inside the nucleus. But most of the knock-on particles will not be able to escape from the nucleus. Qualitatively, therefore, about one extra prong is expected, on the average, to accompany an energetic prong. This figure is consistent with the observed number of star prongs.

A test of this hypothesis would be to calculate the energy and angular distribution of the knock-on particles. The Monte Carlo method of calculation appears to be most suitable, but it will not be attempted in this paper.

IX. Acknowledgments

I should like to thank Drs. W. Barkas, H. Bradner, C. Richman, and R. L. Thornton for their guidance and encouragement, and to express my gratitude to the other members of the Film Program at the Radiation Laboratory for their cooperation and for many fruitful discussions. I

am also indebted to Mr. A. Oliver for the preparation of Figures 9 and 10, and to Miss Betty Summers for the other figures.

X. Mathematical Appendix

A. Least Squares

We wish to minimize the function

$$L = \sum_{n=1}^{N} (y_n - mx_n - b)^2$$

in order to determine the best straight line to fit the points in question, assuming that the error in x_n is small compared to that in y_n. By solving simultaneously the linear equations

$$\frac{\partial L}{\partial m} = 0 \tag{1}$$

$$\frac{\partial L}{\partial b} = 0 \tag{2}$$

The well-known equations for m and b follow:

$$m = \frac{\frac{1}{N}\sum_n x_n y_n - \bar{x}\bar{y}}{D} \tag{3}$$

$$b = \frac{\bar{y} \cdot \frac{1}{N}\sum_n x_n^2 - \bar{x} \cdot \frac{1}{N}\sum_n x_n y_n}{D} \tag{4}$$

where

$$\bar{x} = \frac{1}{N}\sum_n x_n \qquad \bar{y} = \frac{1}{N}\sum_n y_n \tag{5}$$

and

$$D = \frac{1}{N}\Sigma x_n^2 - \bar{x}^2 \tag{6}$$

To estimate the error in x due to an uncertainty δy_n in y, we assume that all δy_n are equal to a constant δy. Then

$$\frac{\partial m}{\partial y_n}\delta y = \frac{\frac{1}{N}x_n - \frac{\bar{x}}{N}}{D}\,\delta y$$

$$\frac{\partial b}{\partial y_n}\delta y = \frac{\frac{1}{N^2}\Sigma x_n^2 - \frac{\bar{x}x_n}{N}}{D}\,\delta y$$

$$(\delta m)^2 = \sum_n \left(\frac{\partial m}{\partial y_n}\right)^2 (\delta y)^2$$

$$= \frac{\frac{1}{N}\Sigma x_n^2 + \bar{x}^2 - 2\bar{x}^2}{ND^2}\,(\delta y)^2$$

$$= \frac{(\delta y)^2}{ND}$$

$$(\delta b)^2 = \Sigma\left(\frac{\partial b}{\partial y_n}\right)^2 (\delta y)^2$$

$$= \frac{\left(\frac{1}{N}\Sigma x_n^2\right)^2 + \frac{\bar{x}^2}{N}\Sigma x_n^2 - \frac{2\bar{x}^2}{N}\Sigma x_n^2}{ND^2}\,(\delta y)^2$$

$$= \frac{\frac{1}{N}\Sigma x_n^2}{ND}\,(\delta y)^2$$

$$= (\delta m)^2 \cdot \frac{1}{N}\Sigma x_n^2$$

$$(\delta x)^2 = \sum_n \left(\frac{\partial x}{\partial m}\frac{\partial m}{\partial y_n} + \frac{\partial x}{\partial b}\frac{\partial b}{\partial y_n}\right)^2 (\delta y)^2; \qquad x = \frac{y-b}{m},\ \frac{\partial x}{\partial m} = \frac{-(y-b)}{m^2},\ \frac{\partial x}{\partial b} = -\frac{1}{m}$$

$$= \left[\left(\frac{y-b}{m^2}\right)^2 \Sigma\left(\frac{\partial m}{\partial y_n}\right)^2 + \frac{1}{m^2}\Sigma\left(\frac{\partial b}{\partial y_n}\right)^2 + \frac{2(y-b)}{m^3}\Sigma\frac{\partial m}{\partial y_n}\frac{\partial b}{\partial y_n}\right](\delta y)^2$$

$$= \left(\frac{y-b}{m^2}\right)^2 (\delta m)^2 + \frac{1}{m^2}\cdot\frac{1}{N}\Sigma x_n^2\,(\delta m)^2$$

$$+ \frac{2(y-b)}{m^3}\sum_n \frac{\frac{1}{N}x_n\cdot\frac{1}{N}\Sigma x_n^2 - \left(\frac{1}{N}\Sigma x_n\right)\bar{x}\cdot x_n - \frac{\bar{x}}{N^2}\Sigma x_n^2 + \frac{\bar{x}^2 x_n}{N}}{\frac{ND^2}{(\delta y)^2}}$$

$$= \left(\frac{\delta m}{m}\right)^2 \left\{x^2 + \frac{1}{N}\Sigma x_n^2 + \frac{2x(\delta y)^2}{m(\delta m)^2}\left[\frac{\bar{x}\cdot\frac{1}{N}\Sigma x_n^2 - \bar{x}\cdot\frac{1}{N}\Sigma x_n^2 - \bar{x}\cdot\frac{1}{N}\Sigma x_n^2 + \bar{x}^3}{ND^2}\right]\right\}$$

$$= \frac{(\delta m)^2}{m^2}\left[\frac{1}{N}\Sigma x_n^2 + x^2 - 2x\bar{x}\right]$$

$$(\delta x)^2 = \frac{(\delta m)^2}{m^2}\left[\frac{1}{N}\Sigma x_n^2 + \left(\frac{y-b}{m}\right)^2 - 2\bar{x}\left(\frac{y-b}{m}\right)\right]$$

$$(\delta x)^2_{min} = (\delta x)^2_{x=\bar{x}} = \frac{(\delta m)^2}{m^2}\left[\frac{1}{N}\sum x_n^2 - \bar{x}^2\right]$$

B. Geometry

It is assumed that the proton is emitted with spherical symmetry. The emulsion has a thickness t before development, and a star is formed at a distance x from the top of the emulsion. A fast proton leaves at an angle ϕ_x with the plane of the emulsion and must have a projection upon the plane of the emulsion of not less than ℓ in order to be counted. No particle within 12μ (before development) of either emulsion surface is included, and no proton all of whose length is within 24μ (before development) of either surface is counted.

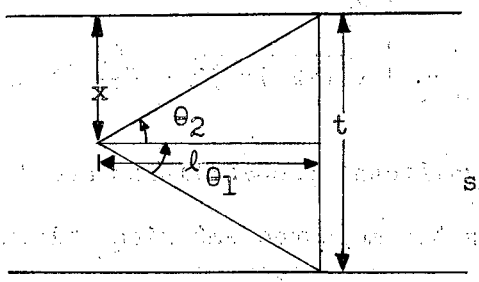

$$\theta_1 = \tan^{-1}\frac{-(t-x)}{\ell} \qquad \theta_2 = \tan^{-1}\frac{x}{\ell}$$

$$\sin\theta_1 = -\frac{t-x}{\sqrt{(t-x)^2+\ell^2}} \qquad \sin\theta_2 = \frac{x}{\sqrt{x^2+\ell^2}}$$

$$P_1 = \text{Prob}\left\{\phi \leq \phi_x \leq \phi + d\phi\right\} = \frac{1}{2}\cos\phi d\phi$$

$$P_2 = \text{Prob}\left\{\theta_1 \leq \phi_x \leq \theta_2\right\} = \frac{1}{2}\int_{\theta_1}^{\theta_2}\cos\phi d\phi = \frac{1}{2}\left[\frac{t-x}{\sqrt{(t-x)^2+\ell^2}} + \frac{x}{\sqrt{x^2+\ell^2}}\right]$$

$$P_3 = \text{Prob}\left\{\begin{matrix}\theta_1 \leq \phi \leq \theta_2 \text{ for} \\ 12 \leq x \leq t-12\end{matrix}\right\} = \int_{12}^{t-12} P_2\frac{dx}{t-24} = \frac{1}{t-24}\int_{12}^{t-12}\frac{xdx}{\sqrt{x^2+\ell^2}}$$

$$= \frac{1}{t-24}\left[\sqrt{(t-12)^2+\ell^2} - \sqrt{(12)^2+\ell^2}\right]$$

$$P_4 = \text{Prob}\left\{0 \leq \phi_x \leq \theta_2\right\} = \frac{1}{2}\int_0^{\theta_2}\cos\phi d\phi = \frac{1}{2}\frac{x}{\sqrt{x^2+\ell^2}}$$

$$P_5 = \text{Prob}\left\{\begin{array}{l} 0 \leq \phi \leq \theta_2 \text{ for } 12 \leq x < 24 \\ \underline{\text{and}} \\ 0 \geq \phi \geq \theta_1 \text{ for } t-24 < x \leq t-12 \end{array}\right\}^*$$

$$= 2\int_{12}^{24} P_4 \frac{dx}{t-24} = \frac{1}{t-24}\left[\sqrt{(24)^2+\ell^2} - \sqrt{(12)^2+\ell^2}\right]$$

$$P_6 = \text{Prob}\left\{\frac{\pi}{4} < \phi \leq \theta_2\right\} \qquad = \frac{1}{2}\int_{\pi/4}^{\theta_2} \cos\phi d\phi = \frac{1}{2}\left[\frac{x}{\sqrt{x^2+\ell^2}} - \frac{\sqrt{2}}{2}\right]$$

$$P_7 = \text{Prob}\left\{\begin{array}{l} \frac{\pi}{4} < \phi \leq \theta_2 \text{ for } \ell < x \leq t-12 \\ \underline{\text{and}} \\ \theta_1 \leq \phi < -\frac{\pi}{4} \text{ for } 12 \leq x < \ell \end{array}\right\}$$

$$= 2\int_{\ell}^{t-12} P_6 \frac{dx}{t-24}$$

$$= \frac{1}{t-24}\left[\int_{\ell}^{t-12} \frac{x dx}{\sqrt{x^2+\ell^2}} - \frac{\sqrt{2}}{2}\int_{\ell}^{t-12} dx\right]$$

$$= \frac{1}{t-24}\left[\sqrt{(t-24)^2+\ell^2} - \frac{\sqrt{2}}{2}(t-12+\ell)\right]$$

In Table VI below, the significant probabilities are listed for each of the plates used. t' is the measured emulsion thickness; it is multiplied by the shrinkage factor of 2.4[22] to get the original thickness t. N is the number of events which occur, while N_{obs} is the number of events actually observed. Obviously, $N_{obs} = P_3N - P_5N - P_7N$.

* For the C-2plate only the case $0 \leq \phi \leq \theta_2$ for $12 \leq x < 24$ is relevant, and P_5 for that plate is 1/2 the value calculated from the expression given.

Table VI

Plate No.	$t'(\mu)$	$t(\mu)$	$\ell(\mu)$	P_3	P_5	P_7	$\frac{N}{N_{obs}} = \frac{1}{P_3-P_5-P_7}$	
22212	85	204	86	0.686	0.014	0.077	$\frac{1}{0.595}$	1.68
22009	75	180	86	0.654	0.016	0.060	$\frac{1}{0.578}$	1.73
22886	99	238	86	0.724	0.006	0.098	$\frac{1}{0.620}$	1.61

C. Standard Deviations

Assume that the grains of a track are uniform in size, spacing, and sensitivity. For the plates used in this study, about 3 grains per micron is a reasonable value. For a 43μ segment, then, there is a maximum number of 129 grains which may be made developable with equal probability. If $\bar{K}$ is the mean number of developed grains per segment, the probability that K grains are developed in a segment is given by the (K + 1)st term of

$$\left[\frac{\bar{K}}{129} + \left(1 - \frac{\bar{K}}{129}\right)\right]^{129}$$

The standard deviation of this distribution is[27]

$$\sigma = \sqrt{129 \cdot \frac{\bar{K}}{129}\left(1 - \frac{\bar{K}}{129}\right)}$$

For a single measurement N, this becomes $\sigma = \sqrt{N\left(1 - \frac{N}{129}\right)}$, as given in Section VI.

If n segments of a track inclined at an angle ∅ have been measured and a mean grain density $\bar{N}$ has been found, the standard deviation of the total number of grains is $\sqrt{n\bar{N}\left(1 - \frac{n\bar{N}}{129n}\right)}$. The corrected number of grains per segment is then $\frac{n\bar{N}}{n}\cos\phi$, and the standard deviation per

segment

$$\sigma_1 = \frac{\sqrt{n\bar{N}\left(1-\frac{\bar{N}}{129}\right)}}{n}\cos\phi = \sqrt{\frac{\bar{N}}{n}\left(1-\frac{\bar{N}}{129}\right)}\cos\phi$$

D. Asymmetry

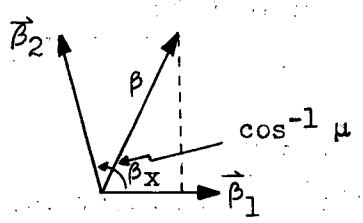

Assume that particles of velocity $\vec{\beta}_2$ are being emitted with spherical symmetry from a nucleus of velocity $\vec{\beta}_1$ ($\beta_1 < \beta_2$) moving in the positive x direction. The x component of the particle velocity in the laboratory system is given by[28] $\beta_x = \frac{\beta_1+\beta_2\mu}{1+\beta_1\beta_2\mu}$, where μ = cosine of the angle between the vectors $\vec{\beta}_1$ and $\vec{\beta}_2$, and β_1 and β_2 are the magnitudes of the vectors $\vec{\beta}_1$ and $\vec{\beta}_2$. β_x will be zero when $\mu = -\frac{\beta_1}{\beta_2}$. If $\mu < -\frac{\beta_1}{\beta_2}$, the particle will be emitted in the negative x direction, while if $\mu > -\frac{\beta_1}{\beta_2}$, the particle will travel in the positive x direction. As a consequence of spherical symmetry, all intervals (μ, $\mu + d\mu$) are equally probable. Therefore the ratio R_{calc} of particles emitted in the direction of the recoiling nucleus to those emitted in the opposite direction is given by

$$R_{calc} = \frac{\int_{-\beta_1/\beta_2}^{1} \frac{\beta_1+\beta_2\mu}{1+\beta_1\beta_2\mu}\,d\mu}{\int_{-1}^{-\beta_1/\beta_2} \frac{\beta_1+\beta_2\mu}{1+\beta_1\beta_2\mu}\,d\mu}$$

$$= \frac{\left\{\frac{1}{\beta_2}\log(1+\beta_1\beta_2 x)+\frac{1}{\beta_1^2\beta_2}\left[1+\beta_1\beta_2 x-\log(1+\beta_1\beta_2 x)\right]\right\}_{-\beta_1/\beta_2}^{1}}{\left\{\frac{1}{\beta_2}\log(1+\beta_1\beta_2 x)+\frac{1}{\beta_1^2\beta_2}\left[1+\beta_1\beta_2 x-\log(1+\beta_1\beta_2 x)\right]\right\}_{-1}^{-\beta_1/\beta_2}}$$

$$R_{calc} = \frac{\beta_2+\beta_1-\frac{1-\beta_1^2}{\beta_1}\log\frac{1-\beta_1^2}{1+\beta_1\beta_2}}{\beta_2-\beta_1+\frac{1-\beta_1^2}{\beta_1}\log\frac{1-\beta_1^2}{1-\beta_1\beta_2}}$$

$$\cong \frac{\beta_2+\beta_1-\frac{1}{\beta_1}\left[-\beta_1^2-\beta_1\beta_2\right]}{\beta_2-\beta_1+\frac{1}{\beta_1}\left[-\beta_1^2+\beta_1\beta_2\right]}, \text{ if } \beta_1,\ \beta_2 << 1$$

$$\therefore R_{calc} = \frac{\beta_2+\beta_1}{\beta_2-\beta_1}$$

XI. References

1. E. Clementel and G. Puppi, Nuovo Cim. 6, 494 (1949).
2. Y. Fujimoto and Y. Yamaguchi, Prog. Theor. Phys. 4, 468 (1949).
3. D. Perkins, Phil.Mag. 40, 601 (1949).
4. M. Menon, H. Muirhead, and O. Rochat, Phil. Mag. 41, 583 (1950).
5. J. Heidmann and L. LePrince-Ringuet, Comptes Rendus 226, 1716 (1948).
6. R. Marshak, Echo Lake Symposium on Cosmic Radiation (1949).
7. Y. Fujimoto, S. Hayakawa, and Y. Yamaguchi, Prog. Theor. Phys. 4, 576 (1949).
8. S. Tamor, Phys. Rev. 77, 412 (1950).
9. F. Adelman, Phys. Rev. 78, 86(A) (1950).
10. W. Cheston and L. Goldfarb, Phys. Rev. 78, 683 (1950).
11. K. Bowker, Phys. Rev. 78, 87(A) (1950).
12. H. Bethe, Phys. Rev. 50, 332 (1936).
13. J. Oppenheimer and R. Serber, Phys. Rev. 50, 391 (1936).
14. J. Bardeen, Phys. Rev. 51, 799 (1937).
15. N. Bohr and F. Kalckar, Kgl Danske Videnskab Selskab, Math-fys. Medd 14, No. 10 (1937).
16. F. Adelman and S. Jones, Science 111, 226 (1950).
17. Y. Fujimoto, K. Takayanagi, and Y. Yamaguchi, Prog. Theor. Phys. 5, 498 (1950).
18. J. Spence, private communication.
19. H. Bradner, F. Smith, W. Barkas, and A. Bishop, Phys. Rev. 77, 462 (1950).
20. F. Smith, W. Barkas, A. Bishop, H. Bradner, and E. Gardner, Phys. Rev. 78, 86(A) (1950).
21. L. Winand, private communication.
22. R. Miller, private communication.

23. B. Rankin, private communication.

24. R. Christian and H. Noyes, Phys. Rev. 79, 85 (1950).

25. S. Ruddlesden and A. Clark, Nature 164, 487 (1949).

26. M. Goldberger, Phys. Rev. 74, 1269 (1948).

27. H. Margenau and G. Murphy, Mathematics of Physics and Chemistry, p. 423 (1943).

28. G. Joos, Theoretical Physics (translated by I. Freeman), p. 232 (1934).

Figure Captions

1. Schematic diagram of apparatus for exposing plates
2. Grain density vs. $\frac{1}{\sqrt{E_p}}$ for various depths in emulsion (G-5 plate No. 22212). E_p is the energy of a proton with the grain density given.
3. Grain density vs. $\frac{1}{\sqrt{E_p}}$ for G-5 plate No. 22212.
4. Correction for depth in emulsion for G-5 plate No. 22212.
5. Grain density vs. $\frac{1}{\sqrt{E_p}}$ for C-2 plate No. 22886.
6. Correction for depth in emulsion for C-2 plate No. 22886.
7. Standard deviation of least squares straight line for G-5 plate No. 22212.
8. Standard deviation of least squares straight line for C-2 plate No. 22886.
9. A. Photomicrograph of meson track taken at various velocities in G-5 plate No. 22009. A proton at the same velocities would have the grain densities and energies shown.
   B. 4-prong meson star, one of whose prongs is a 58 Mev proton.
   C. Meson star with single prong, a 55 Mev proton. An electron is also associated with this event.
10. A. Photomicrograph of meson track taken at various velocities in C-2 plate No. 22886. A proton at the same velocities would have the grain densities and energies shown.
    B. 2-prong meson star, one of whose prongs is a 20-1/2 Mev proton.
    C. 3-prong meson star, one of whose prongs is a 56-1/2 Mev proton.
11. Energy spectrum of emitted protons of energy greater than 20 Mev.
12. Prong spectrum of emitted protons of energy greater than 20 Mev.

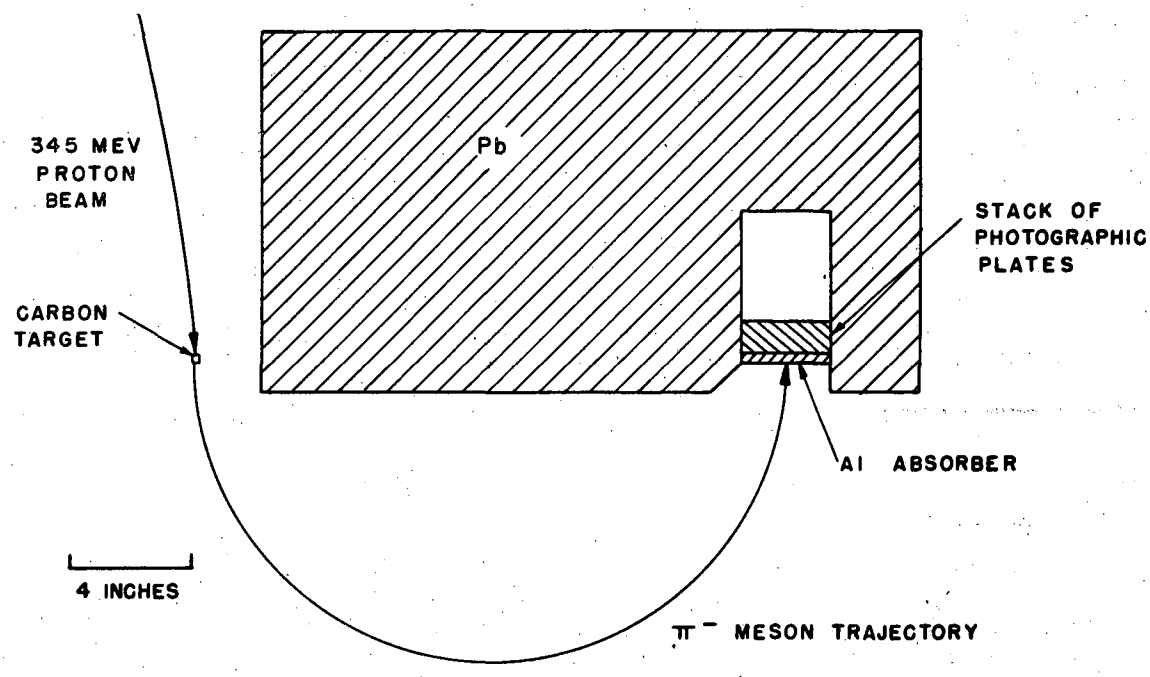
345 MEV
PROTON
BEAM
Pb
STACK OF
PHOTOGRAPHIC
PLATES
CARBON
TARGET
Al ABSORBER
4 INCHES
π⁻ MESON TRAJECTORY

FIG. 1

MU 993

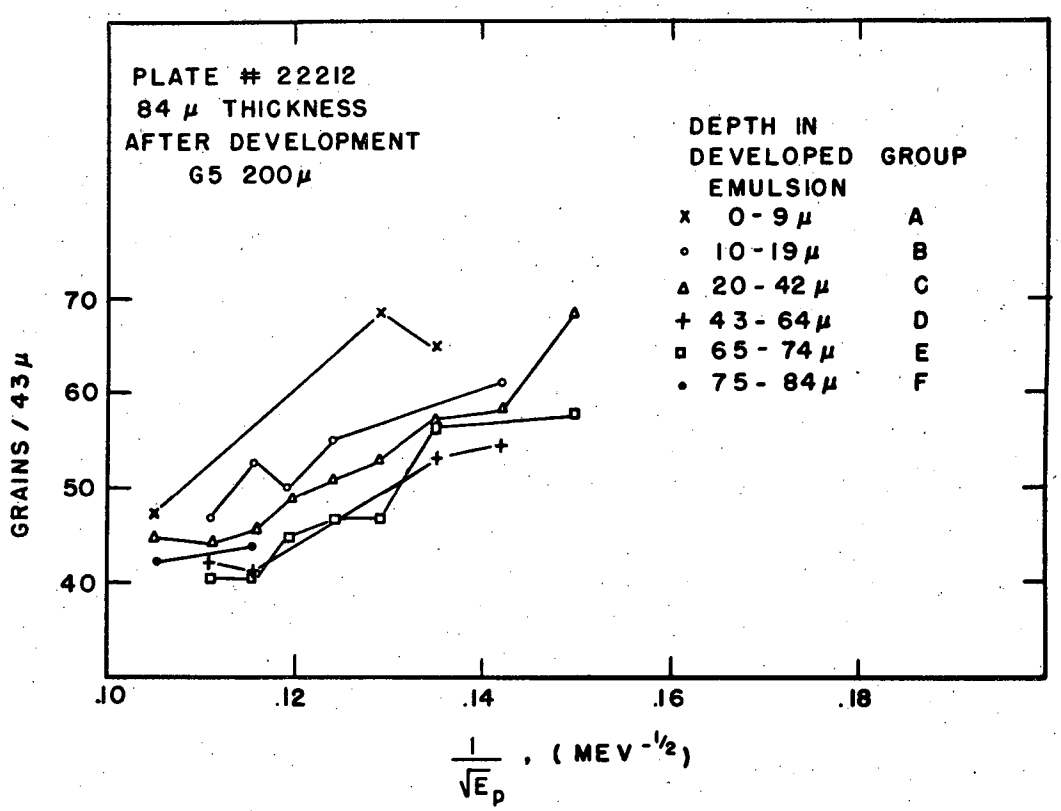
PLATE # 22212
84 μ THICKNESS
AFTER DEVELOPMENT
G5 200μ
DEPTH IN DEVELOPED EMULSION
GROUP
x 0 - 9 μ A
∘ 10 - 19 μ B
Δ 20 - 42 μ C
+ 43 - 64 μ D
□ 65 - 74 μ E
• 75 - 84 μ F
GRAINS / 43 μ
70
60
50
40
.10
.12
.14
.16
.18
1/√E_p , (MEV^-1/2)

FIG. 2

MU 994

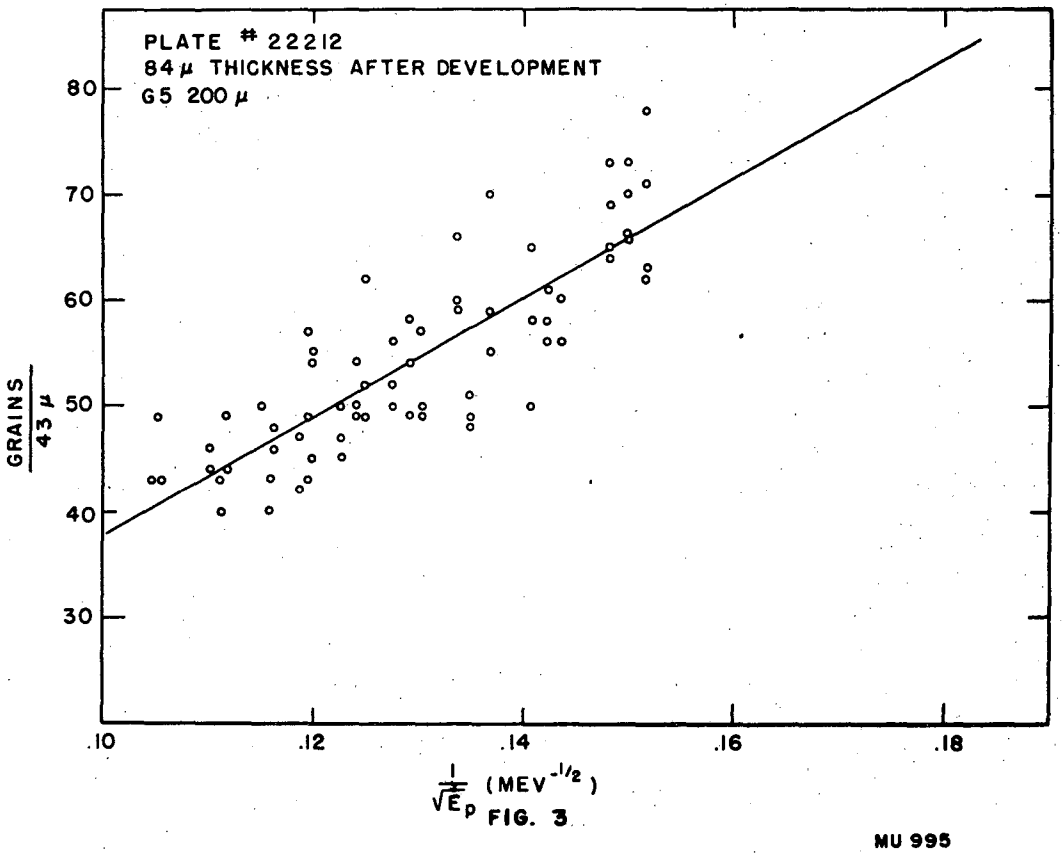
PLATE # 22212
84 μ THICKNESS AFTER DEVELOPMENT
G5 200 μ
80
70
60
50
40
30
GRAINS / 43 μ
.10
.12
.14
.16
.18
1/√E_p (MEV^-1/2)

FIG. 3

MU 995

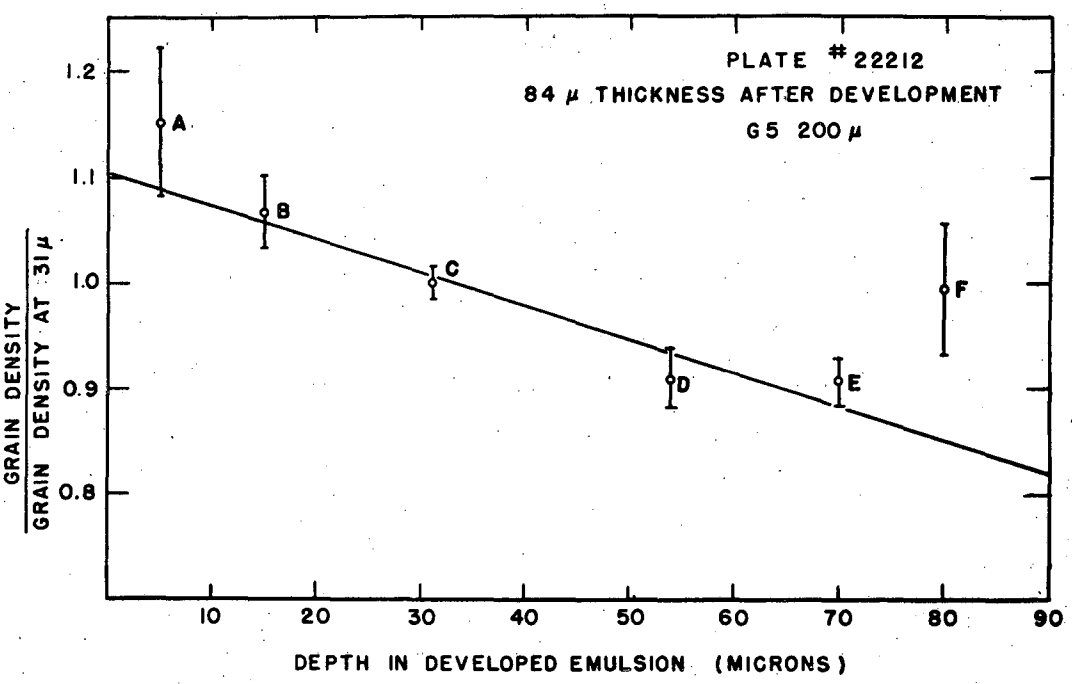
PLATE # 22212
84 μ THICKNESS AFTER DEVELOPMENT
G5 200 μ
A
B
C
D
E
F
1.2
1.1
1.0
0.9
0.8
GRAIN DENSITY / GRAIN DENSITY AT 31 μ
10
20
30
40
50
60
70
80
90
DEPTH IN DEVELOPED EMULSION (MICRONS)

FIG. 4

MU 996

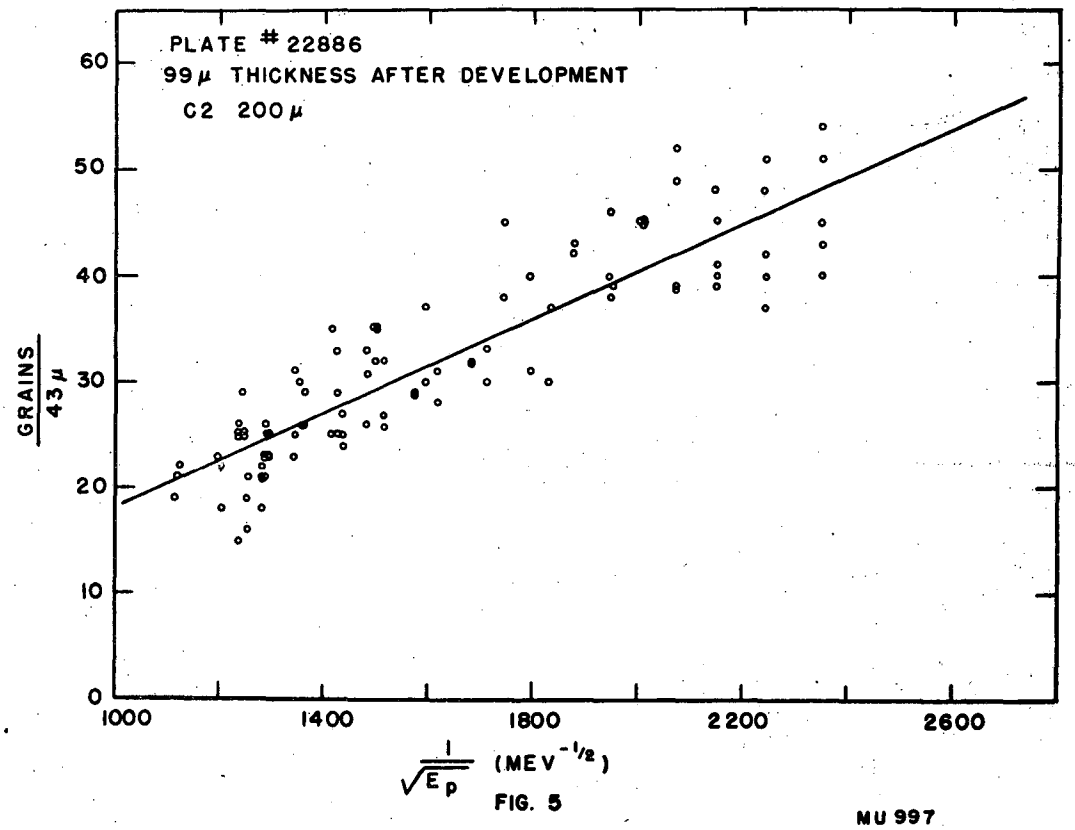
PLATE # 22886
99 μ THICKNESS AFTER DEVELOPMENT
C2 200 μ
GRAINS / 43 μ
0
10
20
30
40
50
60
1000
1400
1800
2200
2600
1/√Ep (MEV^-1/2)

FIG. 5

MU 997

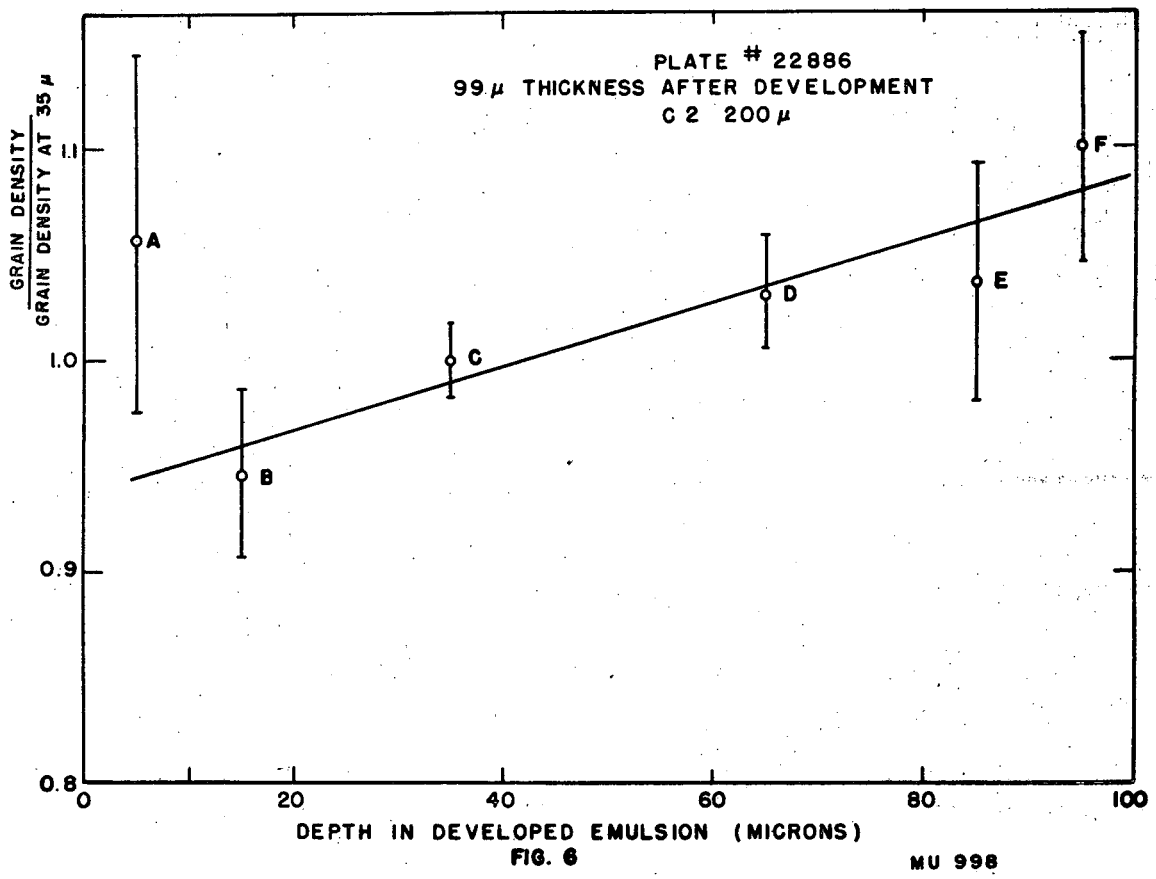
PLATE # 22886
99 μ THICKNESS AFTER DEVELOPMENT
C 2 200 μ
GRAIN DENSITY / GRAIN DENSITY AT 35 μ
1.1
1.0
0.9
0.8
A
B
C
D
E
F
0
20
40
60
80
100
DEPTH IN DEVELOPED EMULSION (MICRONS)

FIG. 6

MU 998

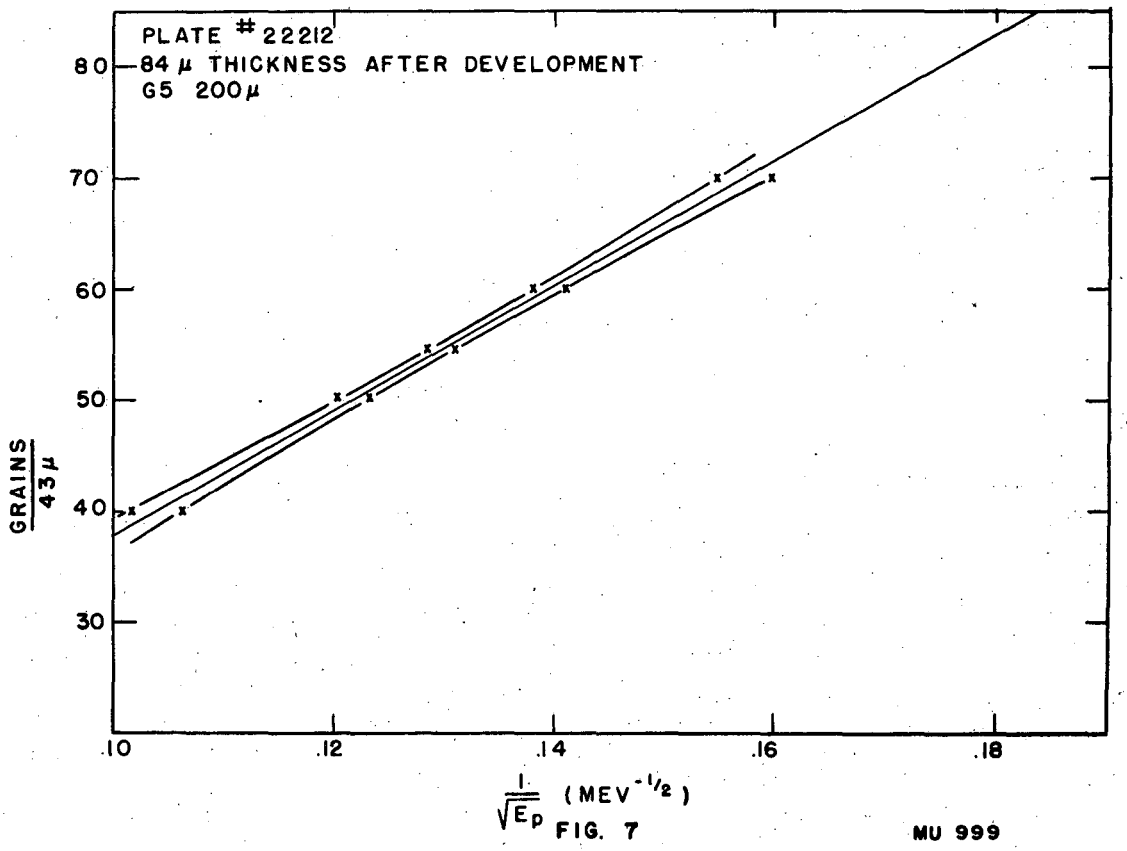
PLATE # 22212
84 μ THICKNESS AFTER DEVELOPMENT
G5 200μ
80
70
60
50
40
30
GRAINS / 43 μ
.10
.12
.14
.16
.18
1/√Ep (MEV^-1/2)

FIG. 7

MU 999

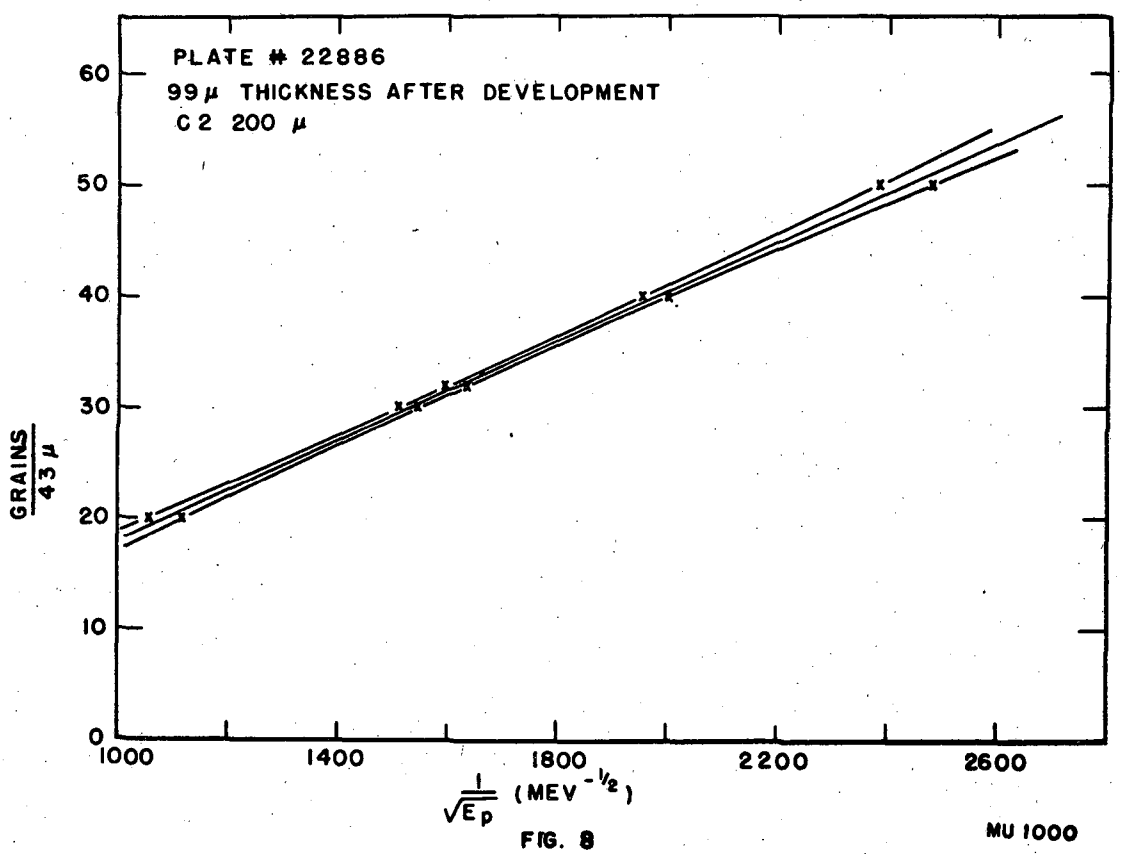
PLATE # 22886
99 μ THICKNESS AFTER DEVELOPMENT
C 2 200 μ
GRAINS / 43 μ
0
10
20
30
40
50
60
1000
1400
1800
2200
2600
1/√Ep (MEV^-1/2)
MU 1000

FIG. 8

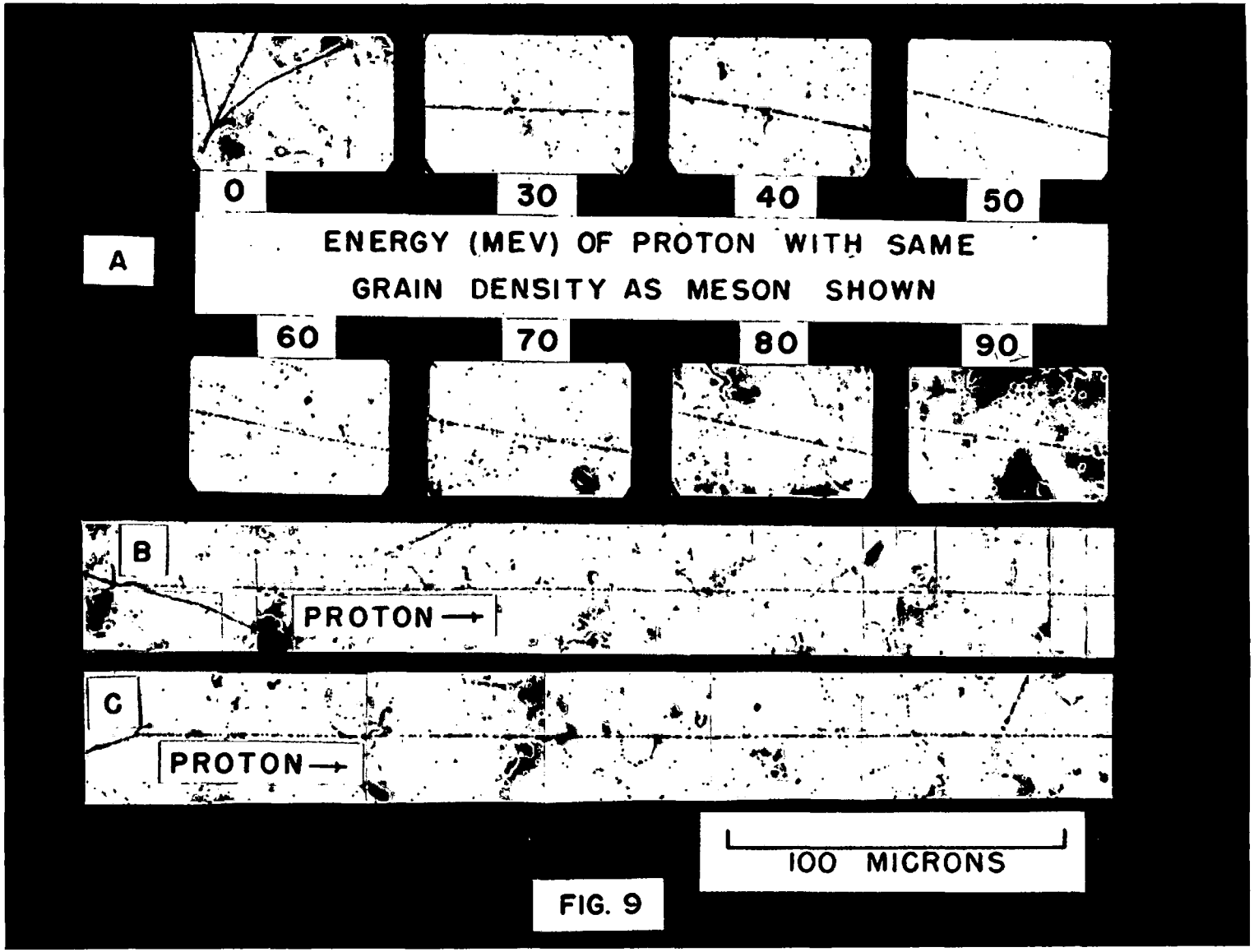
0
30
40
50
A
ENERGY (MEV) OF PROTON WITH SAME
GRAIN DENSITY AS MESON SHOWN
60
70
80
90
B
PROTON
C
PROTON
100 MICRONS

FIG. 9

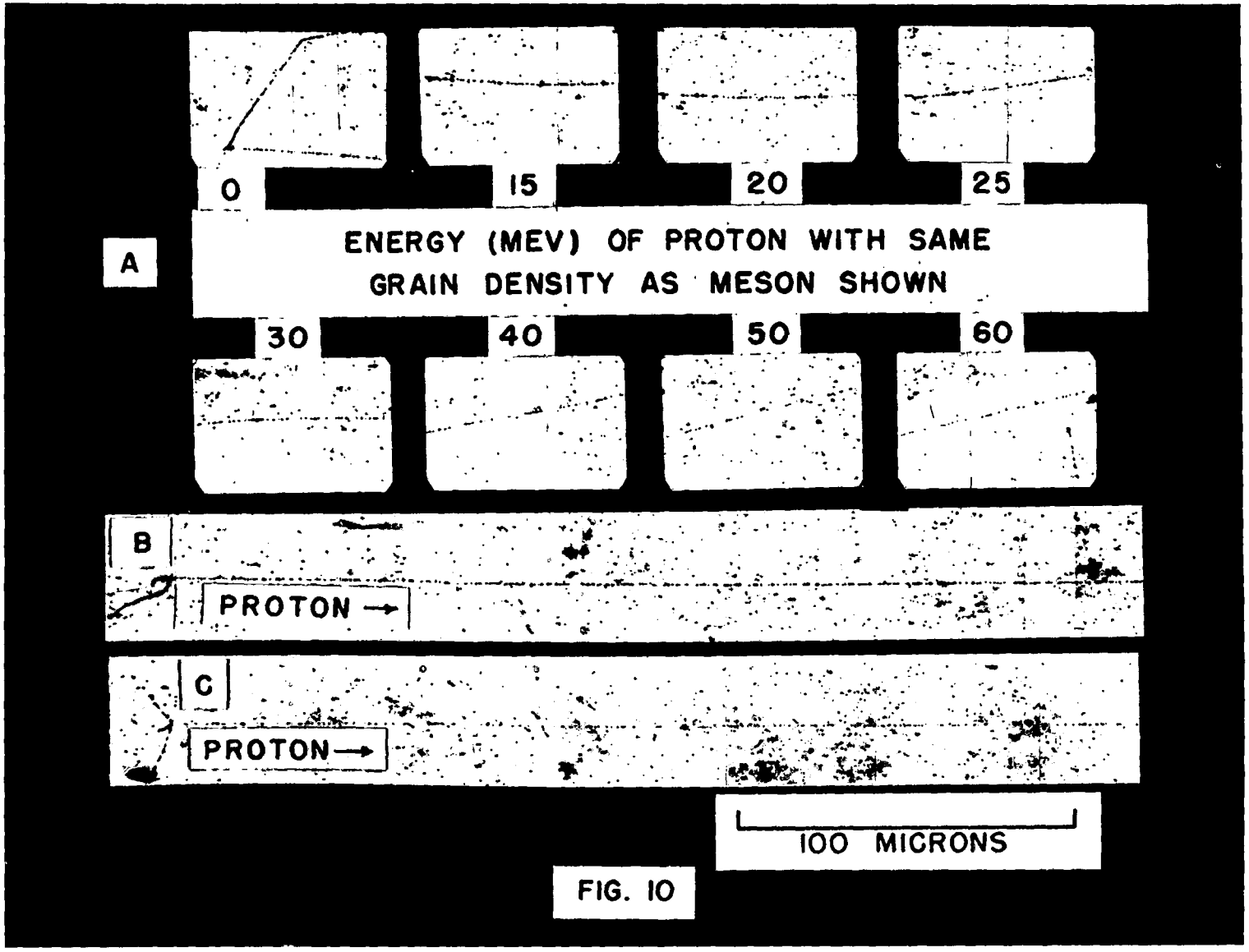

FIG. 10

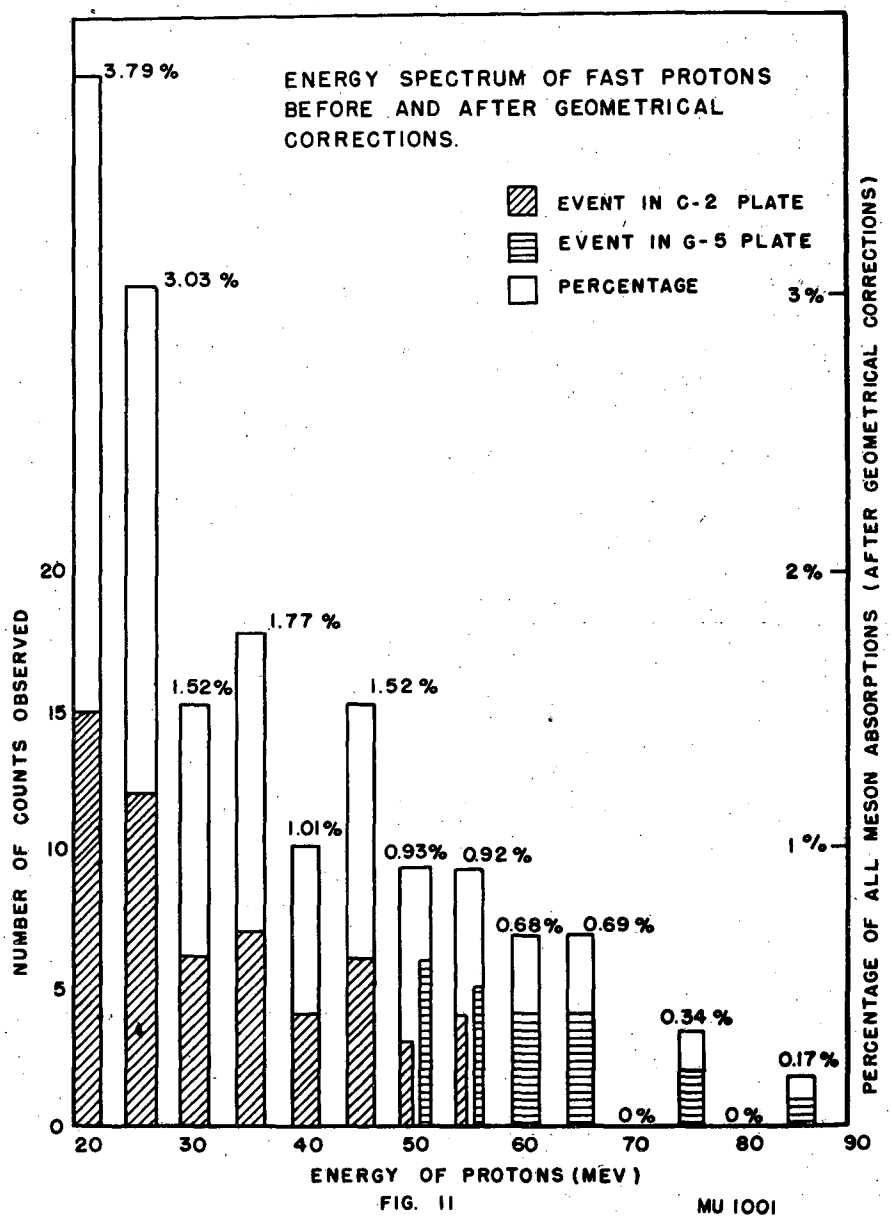

FIG. 11 MU 1001

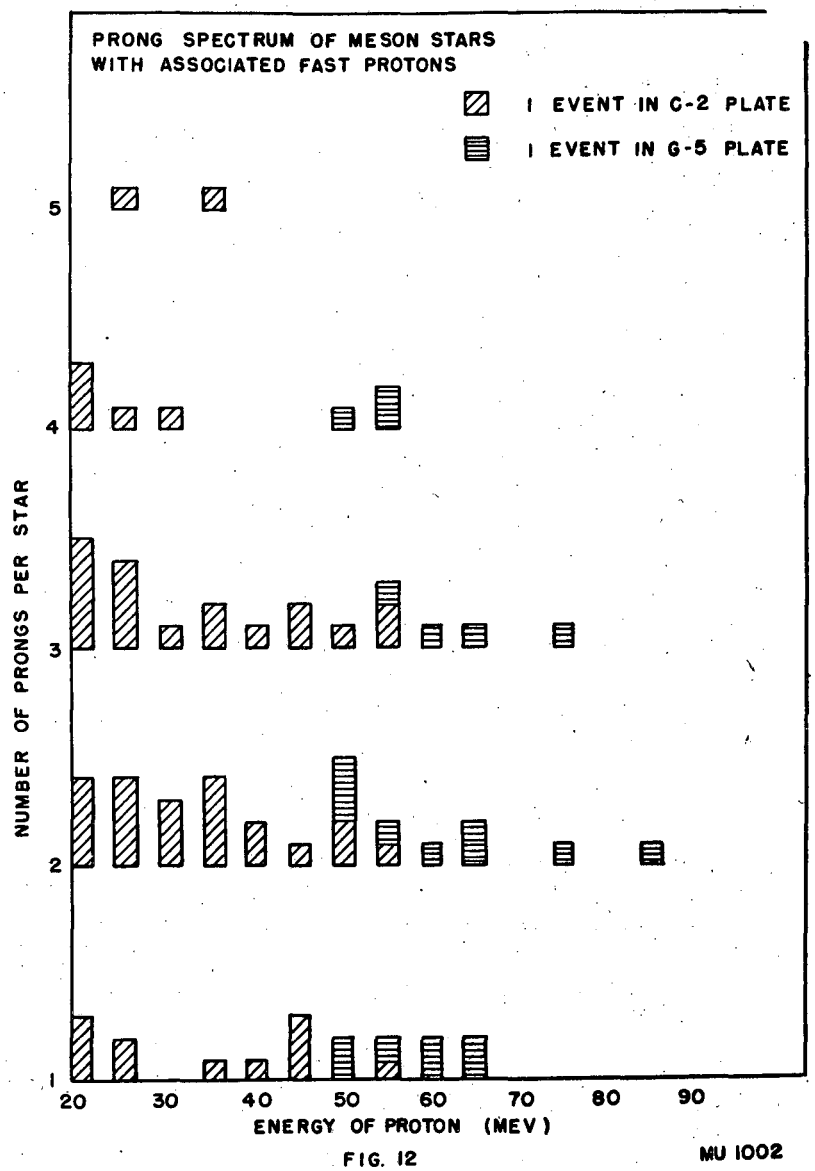

FIG. 12

MU 1002